Eur. Phys. J. A **28**, 277–281 (2006)
DOI 10.1140/epja/i2005-10286-8

THE EUROPEAN PHYSICAL JOURNAL A

Loss of collectivity in ^{79}Rb

R.K. Sinha[1,a], A. Dhal[1], P. Agarwal[2], S. Kumar[2], Monika[3], B.B. Singh[4], R. Kumar[4], P. Bringel[5], A. Neusser[5], R. Kumar[6], K.S. Golda[6], R.P. Singh[6], S. Muralithar[6], N. Madhavan[6], J.J. Das[6], K.S. Thind[3], A.K. Sinha[7], I.M. Govil[4], R.K. Bhowmik[6], J.B. Gupta[8], P.K. Joshi[9], A.K. Jain[2], S.C. Pancholi[6,b], and L. Chaturvedi[1,c]

[1] Physics Department, Banaras Hindu University, Varanasi - 221 005, India
[2] Physics Department, IIT Roorkee, Roorkee - 247 667, India
[3] Physics Department, Guru Nanak Dev University, Amritsar - 143 005, India
[4] Physics Department, Panjab University, Chandigarh - 160 014, India
[5] HISKP, University of Bonn, Germany
[6] Inter University Accelerator Centre (formerly known as NSC), New Delhi - 110 067, India
[7] UGC-DAE Consortium for Scientific Research (formerly known as IUC-DAEF), Kolkata Centre, Kolkata - 700 091, India
[8] Ramjas College, Delhi University, Delhi - 110 007, India
[9] Tata Institute of Fundamental Research, Mumbai - 400 005, India

Received: 13 September 2005 / Revised: 13 June 2006 /
Published online: 20 July 2006 –
Communicated by R. Krücken

Abstract. High-spin states in ^{79}Rb were populated in the reaction ^{63}Cu(^{19}F, p2n)^{79}Rb at E (beam) = 60 MeV. The lifetimes of the excited states of the $\pi g_{\frac{9}{2}}$ positive-parity yrast band and of the $\pi p_{\frac{3}{2}}$ negative-parity band in ^{79}Rb were measured by the Doppler Shift Attenuation Method. The deduced transition quadrupole moments Q_t are found to have a decreasing trend with rotational frequency for both the bands, consistent with those found experimentally in neighbouring nuclei.

PACS. 21.10.Tg Lifetimes – 27.50.+e $59 \leq A \leq 89$

The region of nuclei with $A \approx 80$ is very rich in nuclear phenomena. It contains nuclei having large deformation with very interesting features. These nuclei have low density of single-particle levels and large shell gaps of ≈ 2 MeV at oblate ($\beta_2 \approx -0.3$, N or $Z = 34, 36$) and prolate ($\beta_2 \approx +0.4$, N or $Z = 38, 40$) shapes, exhibiting the dependence of nuclear shapes on proton number, neutron number and on their configuration as well as on spin and lead to shape coexistence effects. This has, therefore, generated a lot of interest towards the study of nuclear shapes in nuclei in this mass region.

The opportunity to investigate highly deformed rotational bands in nuclei to high spins using the high photopeak detection efficiency gamma detector arrays, like Gammasphere and Euroball, has made it possible to discover the phenomenon of band termination [1]. In $A \sim 80$ nuclei, terminating bands have been found in ^{73}Br [2], ^{76}Kr [3] and possibly in ^{81}Y [4,5]. One of the characteristic features of the terminating bands is the observation of a gradual loss of collectivity with spin due to a continuous transition within the band from a collective rotation at low spin to a non-collective single-particle state at maximum spin which can be generated in the same configuration. A loss of collectivity has also been observed in ^{78}Kr [6] and ^{77}Rb [7] for some positive- and negative-parity bands.

The purpose of the present work is to search for such a loss of collectivity with spin in the positive- and the negative-parity bands in ^{79}Rb by measurement of lifetimes of high-spin states using the Doppler Shift Attenuation Method (DSAM). Earlier measurements [8,9] in this nucleus show large errors in the deduced transition quadrupole moments which did not permit any conclusion to be drawn about the possible loss of collectivity.

The levels of ^{79}Rb were populated by the heavy-ion fusion evaporation reaction ^{63}Cu(^{19}F, p2n)^{79}Rb using a 60 MeV ^{19}F beam from the 15 UD Pelletron accelerator at the Inter University Accelerator Centre (IUAC), New Delhi. The target used was the enriched ^{63}Cu of thickness 700 μg/cm^2 with a backing of Ta of thickness 8 mg/cm^2. The γ-rays were detected using the Indian National Gamma Array (INGA), an array consisting of eight Compton-suppressed clover detectors mounted on oppo-

[a] e-mail: rishi_india@rediffmail.com
[b] *Formerly at*: Department of Physics and Astrophysics, Delhi University, Delhi - 110 007, India.
[c] *Present address*: Vice Chancellor, Pandit Ravishankar Shukla University, Raipur - 492010, India.

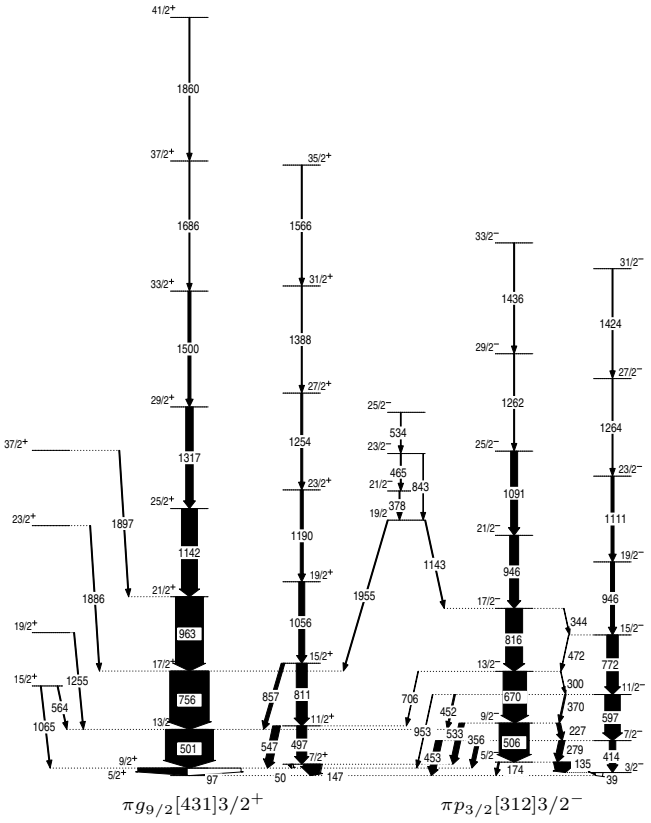

Fig. 1. Partial level scheme of ^{79}Rb [9].

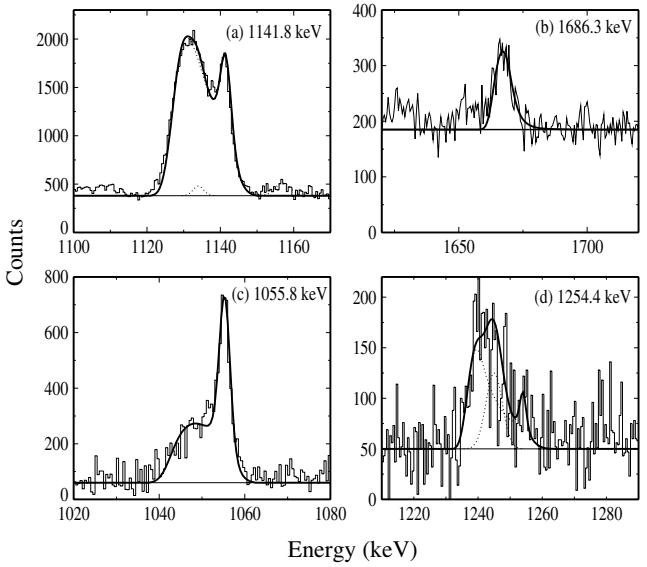

Fig. 2. Experimental and theoretical lineshapes observed for both signature partners of the positive-parity band. (a) and (b) show, respectively, the 1141.8 and 1686.3 keV transition lineshape for the $\alpha = +1/2$ signature band, gate at 501 keV transition, while (c) and (d) show, respectively, the 1055.8 and 1254.4 keV transition lineshape for the $\alpha = -1/2$ signature band, gate at 497 keV transition, for the backward detectors. The contaminant peaks are shown by dotted lines.

site sides of the target chamber making angles of 81° and 141° with respect to the beam direction and tilted at 18° with respect to the horizontal plane. The target-to-detector distance was 24 cm. The total photopeak detection efficiency of the array is $\sim 1.2\%$ at 1.3 MeV γ-ray energy. In the experiment about 850 million γ-γ events were collected. The data from the detectors at backward angle of 141° were used for the lineshape analysis. For the DSAM analysis a single $4\,\mathrm{K} \times 4\,\mathrm{K}$ γ-γ matrix was constructed with a dispersion of 0.5 keV/channel using the program INGASORT [10]. The efficiency calibration was carried out with ^{152}Eu and ^{133}Ba radioactive sources.

The lifetimes of the levels in ^{79}Rb (fig. 1) were estimated by using the LINESHAPE code [11]. This code was used to generate the velocity profile of the recoiling nuclei into the backing material using Monte Carlo technique with a time step of 0.001 ps for 5000 histories of energy losses at different depths. The electron stopping powers of Northcliffe and Schilling [12] corrected for shell effects were used for calculating the energy loss. The lifetime analysis was performed starting with the topmost transition which was assumed to have 100% side-feed via a rotational cascade of five transitions with the same moment of inertia as the in-band transitions. The highest transition in the cascade for which the lineshape was observed was then fitted to the calculated lineshape. The extracted effective lifetime of the topmost excited state from which the above transition decayed, was used as an input parameter to deduce the lifetimes of the lower members of the cascade. The side-feeding intensities of the lower states were obtained from the intensity balance at each level of the cascade. The same side-feeding model of rotational cascade of five transitions, as mentioned above, was used throughout the lifetime analysis. The side-feeding intensities for the positive- and the negative-parity bands were obtained from ref. [9] are mentioned in tables 1 and 2. A 20% variation in the side-feeding intensities was considered in the analysis. In the fitting procedure, a χ^2 minimization of the fit for a) Q_t, the transition quadrupole moment for the transition under consideration and b) Q_t(SF), the transition quadrupole moment of the side-feeding transition to that level, was carried out. After obtaining the Q_t and Q_t(SF) corresponding to a state, this method of analysis was also applied to the level(s) below. The uncertainties in the lifetimes were derived from the behaviour of the χ^2 fit in the vicinity of the minimum. A 15% systematic error due mainly from the uncertainty in the nuclear stopping powers was incorporated in the lifetime values. For every observed lineshape, in-band and side-feeding lifetimes, background parameters, and the intensities of the contaminant peaks were allowed to vary. The uncertainty involved in the lifetimes and consequently in the transition quadrupole moments were determined by the statistical method using the subroutine MINOS [13].

The observed lineshapes were obtained by gating below the transition of interest. Figure 2 shows the observed lineshapes and their simulated lineshapes for the 1141.8, 1686.3, 1055.8 and 1254.4 keV transitions, in the positive-parity bands and in fig. 3 for the 946.3, 1436.4, 1111.1 and 1423.6 keV transitions in the negative-parity bands.

Table 1. Experimental values of lifetimes and transition quadrupole moments Q_t for the positive-parity $\pi g_{\frac{9}{2}}[431]\frac{3}{2}^+$ yrast band in ^{79}Rb. A 15% systematic error due mainly from the uncertainty in the nuclear stopping powers was incorporated in the lifetime values.

E (level) (keV)	I^π ($\hbar$)	E_γ (keV)	τ (ps) ref. [8]	τ (ps) ref. [9]	τ (ps)	Q_t (eb)	Q_t(SF) (eb)	I_γ(SF) [a] (relative)
$\alpha = +1/2$ band								
597.5	$\frac{13}{2}^+$	500.8	11.9(6)					
1353.2	$\frac{17}{2}^+$	755.7	1.2(2)	1.0(3)	1.11(43)	3.10(46)	4.00	30
2315.7	$\frac{21}{2}^+$	962.5	0.49(10)	0.26(3)	0.37(14)	2.85(43)	3.15	29
3457.5	$\frac{25}{2}^+$	1141.8	0.24(6)	0.14(3)	0.29(11)	2.07(31)	3.16	22
4774.3	$\frac{29}{2}^+$	1316.8	< 0.3	0.06(2)	0.10(4)	2.40(36)	6.50	11
6274.5	$\frac{33}{2}^+$	1500.2		< 0.10	0.16(7)	1.36(20)	5.34	5
7960.8	$\frac{37}{2}^+$	1686.3			0.03(1)	2.33(40)	6.15	2
9820.8	$\frac{41}{2}^+$	1860.0			< 0.04	> 1.47		
$\alpha = -1/2$ band								
643.9	$\frac{11}{2}^+$	496.9	8.2(4)					
1454.4	$\frac{15}{2}^+$	810.5	1.3(2)		1.39(56)	2.37(36)	5.75	25
2510.2	$\frac{19}{2}^+$	1055.8		0.23(6)	0.43(16)	2.13(32)	3.78	17
3699.8	$\frac{23}{2}^+$	1189.6		0.14(3)	0.26(10)	2.00(32)	2.82	10
4954.2	$\frac{27}{2}^+$	1254.4		< 0.23	0.13(5)	2.40(37)	4.00	5
6342.3	$\frac{31}{2}^+$	1388.1			< 0.22	> 1.45		

[a] From measured relative γ-ray intensities [9], normalised to $I(755\gamma) = 100$.

Table 2. Experimental values of lifetimes and transition quadrupole moments Q_t for the negative-parity $\pi p_{\frac{3}{2}}[312]\frac{3}{2}^-$ band in ^{79}Rb. A 15% systematic error due mainly from the uncertainty in the nuclear stopping powers was incorporated in the lifetime values.

E (level) (keV)	I^π ($\hbar$)	E_γ (keV)	τ (ps) ref. [8]	τ (ps) ref. [9]	τ (ps)	Q_t (eb)	Q_t(SF) (eb)	I_γ(SF) [a] (relative)
$\alpha = +1/2$ band								
679.9	$\frac{9}{2}^-$	505.8	9.3(25)					
1349.4	$\frac{13}{2}^-$	669.5	1.9(4)		1.50(59)	3.79(57)	5.00	21
2165.1	$\frac{17}{2}^-$	815.7	0.75(20)	0.53(15)	0.52(28)	3.73(56)	3.12	21
3111.4	$\frac{21}{2}^-$	946.3	0.35(10)	0.23(4)	0.39(15)	2.89(43)	3.46	26
4202.0	$\frac{25}{2}^-$	1090.6	0.2(1)	0.12(4)	0.20(8)	2.77(41)	4.12	6
5463.9	$\frac{29}{2}^-$	1261.9		< 0.21	0.10(4)	2.64(40)	6.09	6
6900.3	$\frac{33}{2}^-$	1436.5			< 0.13	> 1.71		
$\alpha = -1/2$ band								
1822.1	$\frac{15}{2}^-$	772.0			1.01(38)	3.15(47)	4.07	49
2767.8	$\frac{19}{2}^-$	945.7		0.28(7)	0.47(18)	2.68(40)	4.24	24
3878.9	$\frac{23}{2}^-$	1111.1		0.15(3)	0.32(12)	2.14(32)	4.65	12
5463.9	$\frac{27}{2}^-$	1263.5		< 0.17	0.30(12)	1.57(23)	5.00	5
6566.0	$\frac{31}{2}^-$	1423.6			< 0.18	> 1.47		

[a] From measured relative γ-ray intensities [9], normalised to $I(755\gamma) = 100$.

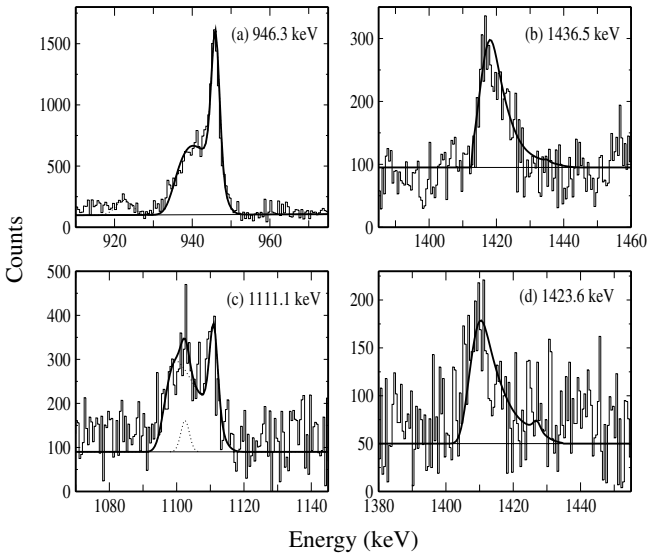

Fig. 3. Experimental and theoretical lineshapes observed for both signature partners of the negative-parity band. (a) and (b) show, respectively, the 946.3 and 1436.4 keV transition lineshape for the $\alpha = +1/2$ signature band, gate at 506 keV transition, while (c) and (d) show, respectively, the 1111.1 and 1423.6 keV transition lineshape for the $\alpha = -1/2$ signature band, gate at 597 keV transition, for the backward detectors. The contaminant peaks are shown by dotted lines.

To check the consistency of the data, we have determined the lineshapes (not shown) of the 963 keV transition in the positive-parity band by gating below and above the transition of interest. The lifetime values so determined in this transition are in good agreement with each other.

Tables 1 and 2 give the values of the lifetimes τ, and of the transition quadrupole moments Q_t for both positive- and negative-parity bands, respectively, as obtained in the present work. In each cascade only an upper limit for the lifetime could be estabilished for the highest state as the correct feeding to that state could not be established. Taking an average of Q_t for the first two transitions for the favoured partners of the positive-parity and of the negative-parity bands, respectively, and using the formula given below

$$Q_t = 3ZeR_0^2\beta_2(1 + 0.16\beta_2)/\sqrt{5\pi} \qquad (1)$$

(axial symmetric, $\gamma = 0$), we find the following deformation parameters: $\beta_2(\pi = +, \alpha = +1/2) = 0.34$ and $\beta_2(\pi = -, \alpha = +1/2) = 0.41$ for these bands.

Figures 4 and 5 are the plots of the transition quadrupole moments, Q_t, deduced from lifetime measurements (present work) *vs.* rotational frequency, $\hbar\omega$, for the positive-parity decoupled $\pi g_{\frac{9}{2}}[431]\frac{3}{2}^+$ yrast band and the negative-parity decoupled $\pi p_{\frac{3}{2}}[312]\frac{3}{2}^-$ band, respectively, in ^{79}Rb. As is seen in the figures, Q_t decreases with $\hbar\omega$ in both the bands for the favoured and the unfavoured partners. However, the decrease appears more regular in the negative-parity band than in the positive-parity band.

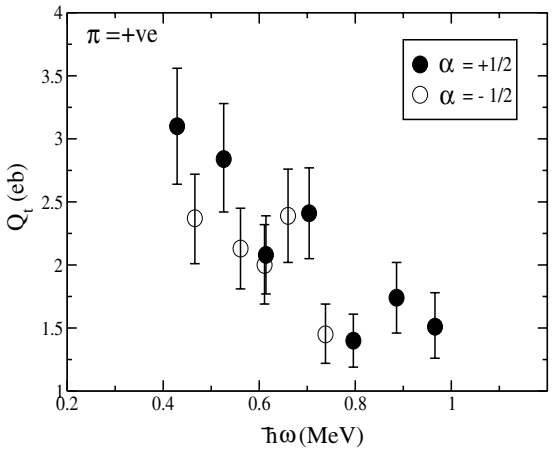

Fig. 4. Plot of Q_t *vs.* $\hbar\omega$ for the positive-parity band (present work).

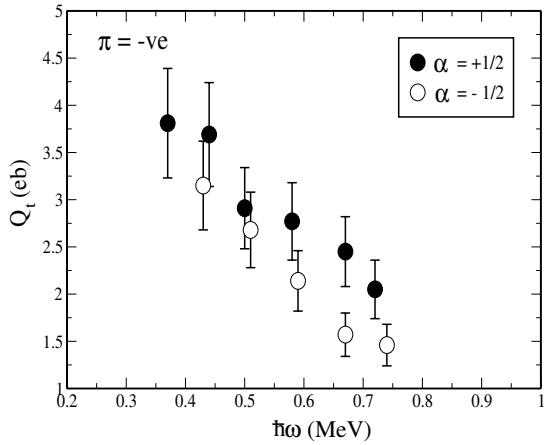

Fig. 5. Plot of Q_t *vs.* $\hbar\omega$ for the negative-parity band (present work).

Extensive theoretical study of the positive-parity $\pi g_{\frac{9}{2}}$ favoured and the unfavoured bands in ^{79}Rb has been done in [14]. The Total Routhian Surface (TRS) calculations have been performed by them for the two lowest $\pi g_{\frac{9}{2}}$ configurations at frequencies below and above the alignment of a neutron $g_{\frac{9}{2}}$ pair at $\hbar\omega \approx 0.6$ MeV. The results show that at low rotational frequencies, both the signature partners have similar prolate deformations ($\beta_2 \approx 0.33$). At rotational frequencies above the neutron alignment, there are two minima with similar β_2 values (≈ 0.29), one having $\gamma \approx -10°$, the other $\gamma \approx -50°$ depending upon the signature. The deepest minimum is found at $\gamma \approx -10°$ in the favoured signature but at $\gamma \approx -50°$ in the unfavoured signature. The observed loss of collectivity in the $\pi g_{\frac{9}{2}}$ unfavoured signature may possibly be attributed to the shape change above band crossing, although there is no explanation for the observed loss of collectivity in the favoured-signature partner band.

The TRS calculations for the negative-parity $\pi p_{\frac{3}{2}}$ bands have been performed in [9]. At low rotational frequencies, the shapes are predicted to be nearly prolate

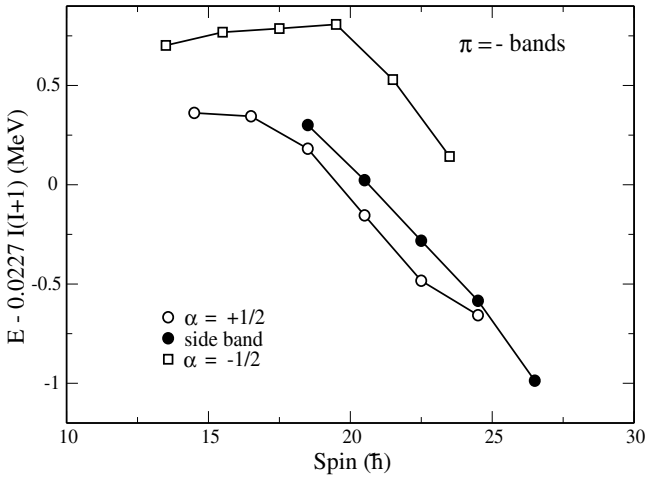

Fig. 6. Energies (from ref. [15]) of the negative-parity $\pi p_{\frac{3}{2}}$ band in ^{79}Rb relative to an $I(I+1)$ rigid-rotor reference *vs.* spin.

($\beta_2 \approx 0.35, \gamma \sim -10°$) which changes to triaxial ($\beta_2 \approx 0.21, \gamma \sim -30°$) at a rotational frequency of 0.691 MeV. The observed fall in Q_t with rotational frequency (fig. 5) for the two signatures of the negative-parity bands may be thought to occur due to the predicted shape changes after the alignments of the $\pi g_{\frac{9}{2}}$ proton pair followed by the $\nu g_{\frac{9}{2}}$ neutron pair alignment [15]. An alternative explanation for the loss of collectivity could be in terms of the band termination phenomenon. In a rotational band built on a specific configuration, the total angular momentum content is limited which gradually gets exhausted up to the maximum spin, $I_{\max}$. The band eventually terminates at the maximum spin in a fully aligned state (terminating state) of single-particle nature. The nuclear shape starts as prolate collective and, with increase in spin, gradually traces a path through a triaxial plane to a non-collective state. Thus, there is a gradual loss of collectivity with increasing spin.

In fig. 6, energies (from ref. [15]) of the excited states in the negative-parity $\pi p_{\frac{3}{2}}$ bands in ^{79}Rb relative to an $I(I+1)$ rigid-rotor reference are plotted *vs.* spin. The negative-parity bands show the familiar trend observed for terminating bands. The data points have not been obtained [15] upto the minima and beyond, in spin, in the plots. This makes it difficult to utilize the configuration-dependent Cranked Nilsson-Strutinsky (CNS) approach, based on the cranked Nilsson potential, to determine the exact configurations for the bands. Band configurations can be specified with respect to a $^{56}_{28}$Ni$_{28}$ core plus 9 active valence protons and 14 active valence neutrons. The distribution of particles and holes and their excitations can be considered within the $N = 3, p_{\frac{3}{2}}, f_{\frac{5}{2}}, p_{\frac{1}{2}}$ and the $N = 4$, $g_{\frac{9}{2}}$ orbitals. As the number of possible proton and neutron configurations are many, it is difficult to use the $I^{\rm p}_{\max} + I^{\rm n}_{\max}$ criteria to arrive at the possible terminating-state spins for the bands. It can, however, only be conjectured that the observed states in the negative-parity bands are several transitions below the terminating states. Further experimental investigations to higher-spin states than observed hitherto [15] are needed to discover the band termination, if present, in this nucleus.

We are thankful to the UGC, New Delhi, for financial support for this project and also thankful to the operational staff of the Pelletron accelerator at IUAC, New Delhi, for smooth operation of the accelerator during the experiment. The help of target laboratory personnel of IUAC is highly acknowledged. The authors would like to thank all the participants in the joint national collaboration to setup INGA at IUAC, New Delhi.

References

1. A.V. Afanasjev *et al.*, Phys. Rep. **322**, 1 (1999).
2. C. Plettner *et al.*, Phys. Rev. C **62**, 014313 (2000).
3. J.J. Valiente-Dobon *et al.*, Phys. Rev. C **71**, 034311 (2005).
4. H. Schnare *et al.*, Phys. Rev. C **56**, 729 (1997).
5. R.A. Kaye *et al.*, Phys. Rev. C **66**, 054305 (2002).
6. A. Dhal *et al.*, Eur. Phys. J. A **27**, 33 (2006).
7. A. Harder *et al.*, Phys. Rev. C **55**, 1680 (1997).
8. J. Panqueva *et al.*, Nucl. Phys. A **389**, 424 (1982).
9. J.W. Holcomb *et al.*, Phys. Rev. C **48**, 1020 (1993).
10. Ranjan Bhowmik, NSC, private communication.
11. J.C. Wells *et al.*, ORNL Physics Division Progress, report No. ORNL-6689, September 30, 1991.
12. L.C. Northcliffe *et al.*, Nucl. Data. Tables **7**, 233 (1970).
13. F. James *et al.*, Comput. Phys. Commun. **10**, 343 (1975)
14. R. Bengtsson *et al.*, Nucl. Phys. A **528**, 215 (1991).
15. D.H. Smalley *et al.*, Nucl. Phys. A **611**, 96 (1996).